STATISTICAL ANALYSIS OF 168 BILATERAL SUBTHALAMIC NUCLEUS IMPLANTATIONS BY MEANS OF THE PROBABILISTIC FUNCTIONAL ATLAS

Wieslaw L. Nowinski, D.Sc., Ph.D.

Biomedical Imaging Laboratory, Institute for Infocomm Research, Singapore, Singapore

Dmitry Belov, Ph.D.

Biomedical Imaging Laboratory, Institute for Infocomm Research, Singapore, Singapore

Pierre Pollak, M.D.

Department of Neurology, University Hospital of Grenoble, Grenoble, France

Alim-Louis Benabid, M.D., Ph.D.

Neurosurgery, Institut National de la Santé et de la Recherche Médicale, University Hospital of Grenoble, Grenoble, France

Reprint requests:
Wieslaw L. Nowinski, D.Sc., Ph.D.,
Biomedical Imaging Laboratory,
Institute for Infocomm Research,
21, Heng Mui Keng Terrace,
Singapore 119613, Singapore
Email: wieslaw@sbic.a-star.edu.sg

Received, November 13, 2003.
Accepted, August 30, 2004.

OBJECTIVE: Statistical analysis of patients previously operated on may improve our methods of performing subsequent surgical procedures. In this article, we introduce a method for studying the functional properties of cerebral structures from electrophysiological and neuroimaging data by using the probabilistic functional atlas (PFA). The PFA provides a spatial distribution of the clinically most effective contacts normalized to a common space. This distribution is converted into a probability function for a given point in space to be inside an effective contact. The PFA was used to analyze spatial properties of the functional subthalamic nucleus (STN), defined as the spatial volume corresponding to the distribution of effective contacts. These results may potentially be useful in planning subthalamic implantation of electrodes.

METHODS: In all, 168 bilateral subthalamic stimulations were examined. An algorithm was developed for converting these data into the PFA. The PFA for the STN (here called "atlas") was calculated with 0.25-mm^3 resolution, and several features characterizing the left and right STN were studied. The analysis was performed with and without lateral compensation against the width of the third ventricle. The key feature introduced here used for analysis of the functional STN is a (probabilistic) functional volume of structure (defined for a given probability as the volume of a region whose every point has a probability equal to or greater than this given probability).

RESULTS: The analysis has been performed for two situations: with and without lateral compensation against the width of the third ventricle. Without lateral compensation, the differences between the mean values and standard deviations of their barycenter coordinates for the left and right functional STNs are 0.31 and 0.18 mm, respectively. The left STN and right STN exhibit differences in functional volume size and probability distribution. The entire functional volume is 240 mm^3 for the left and 229 mm^3 for the right STN. A more prominent difference exists in the region of high probabilities (0.7 or higher), called "hot STN." The volume of the left hot STN is 5.52 mm^3, whereas that of the right is 3.92 mm^3. The left hot STN is 1.41 times bigger and 20% more dense than the right hot STN. For a given probability, the corresponding functional volume for the left hot STN is up to 43 times larger than that for the right STN. Practically speaking, lateral compensation does not change these results qualitatively. Quantitatively, differentiation between the left and right STNs is lower. For instance, for a given probability, the corresponding functional volume for the left hot STN is only up to 11 times larger than that for the right one. In either situation (i.e., with and without lateral compensation), the size of the hot STN in relation to the whole STN remains very small (1–2%). In addition, statistical analysis shows that in either situation, the means of the left and right functional STNs are significantly different.

CONCLUSION: PFA-based planning may be superior to the current practice of using anatomic atlases that provide delineation of the target structure only, because it is more precise and provides a unique target point in the stereotactic space. This best stereotactic target is the point in the individualized atlas with the highest probability,

(continued)

meaning the highest probability of having the best target on the basis of the patients previously operated on. This best target is located in the hot STN, the size of which determines the precision of targeting. Because the size of the hot STN in comparison to the whole STN remains very small (1–2%) independent of whether or not lateral compensation is applied, target planning and execution have to be performed with high precision. The methodology presented, based on the PFA and on the functional volume, is general and can be applied to other structures and data sets. As numerous centers keep gathering large amounts of electrophysiological human and animal data, this work may facilitate opening new avenues in exploiting these data.

KEY WORDS: Brain atlas, Electrophysiology, Probabilistic functional atlas, Statistical analysis, Stereotactic and functional neurosurgery, Subthalamic nucleus

Neurosurgery 57[ONS Suppl 3]:ONS-319–ONS-330, 2005 DOI: 10.1227/01.NEU.0000180960.75347.11

The subthalamic nucleus (STN) is a nucleus of the basal ganglia involved in motor control; it also has associative and limbic components. It has the shape of an almond, is located ventral to the thalamus and medial to the internal capsule, and has reciprocal connections with numerous cortical and subcortical structures, particularly the globus pallidus (*Fig. 1A*). The growing interest in the STN is related to the role it plays in the treatment of Parkinson's disease (PD). Its stimulation at high frequency (or even its ablation) improves the symptoms of PD by suppressing its abnormally increased output and restoring activity of the motor cortex (19). Deep brain stimulation, preferred over therapeutic lesioning, offers an adaptive treatment, reducing morbidity and providing a reversible lesion-mimicking effect. Bilateral stimulation of the STN in PD patients is a promising surgical technique (1–3, 5, 12). It produces a dramatic reversal in all cardinal motor signs in PD patients who are off their medications and offers improvements in the on-medication state. The rationale for choosing STN as a surgical target in PD is based on its abnormal activity in the parkinsonian state and its unique position to affect the neuronal activity of the globus pallidus interna and the substantia nigra pars reticulata as depicted by the models of basal ganglia circuitry and pathophysiology (7).

Targeting in functional neurosurgery is complicated by the individual variations. The initial anatomic target can be identified directly on T2-weighted magnetic resonance imaging (MRI) sections (*Fig. 1B*) or can be defined by use of a high-resolution deformable brain atlas (13) (*Fig. 1C–E*). The anatomic target must then be confirmed by intraoperative electrophysiological findings, including microrecording as well as stimulation. After identification of the target, the microelectrode is replaced by a permanent deep brain simulation electrode bearing four cylindrical contacts (1.27 mm in diameter, 1.5 mm in height) separated by gaps of 1.5 mm (Medtronic 3387) or of 0.5 mm (Medtronic 3389) (Medtronic, Inc., Minneapolis, MN). Several electrodes may be inserted unilaterally or bilaterally, providing vast information about the functional location of cerebral structures. By collecting data from a series of patients clinically followed up, a probabilistic atlas showing a functional distribution of cerebral structures can be constructed (17) and new knowledge can be extracted from it. In

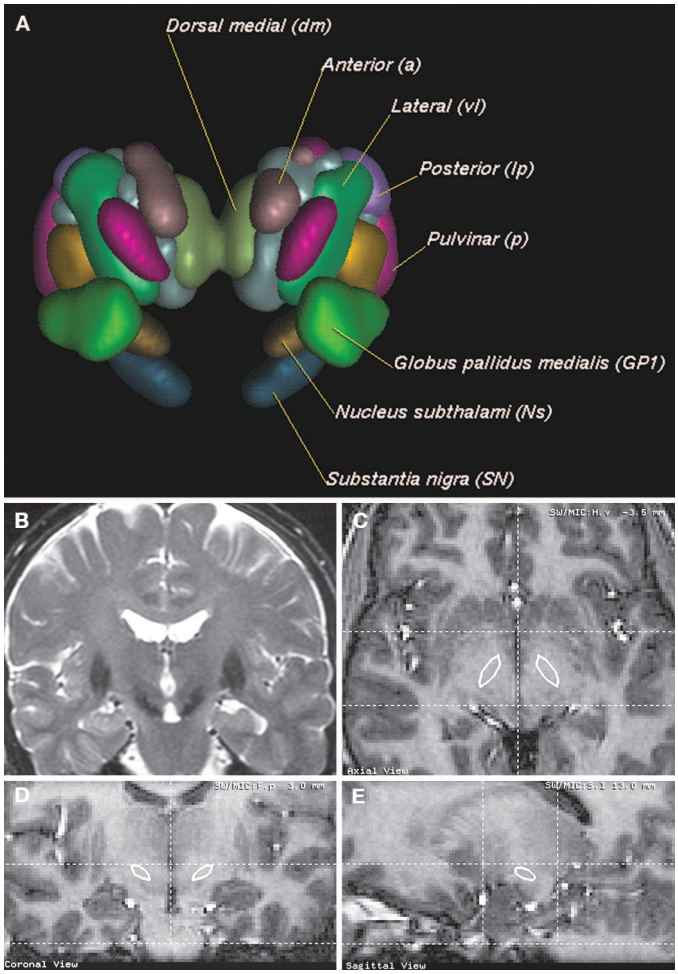

FIGURE 1. *Anatomic STN.* A, *three-dimensional models of the STN (labeled as the* Nucleus subthalami*) along with surrounding structures: globus pallidus interna, substantia nigra, and thalamic nuclei;* B, *T2-weighted MRI coronal scan with the STN;* C–E, *STN contoured by means of a brain atlas on axial* (C), *coronal* (D), *and sagittal* (E) *T1-weighted MRI views along with the reference lines passing through the AC and PC.*

this study, only one contact of each left and right electrode is activated, the contact being connected to the negative (cathodal) pole of the implanted stimulator, the case of which serves as the positive (anodal) pole. The spatial distribution of the clinically effective contacts is represented on each side by a cluster of contacts, which is converted into a spatial probabilistic distribution, representing the probability that a given point in space could be included within a clinically effective contact.

In this study, a probabilistic functional atlas (PFA) has been constructed for the STN from 168 bilateral subthalamic stimulations, and its statistical analysis has been performed. Several features have been studied, including mean value (MV), standard deviation (SD), and volume (V) for the left and right functional STN (STNL and STNR). The analysis has been performed in two situations: 1) compensating the value of the electrode laterality against the width of the third ventricle and 2) without lateral compensation.

MATERIALS AND METHODS

The method contains three major steps: 1) acquisition of electrophysiological, neuroimaging, and neurological assessment data for 168 bilateral subthalamic stimulations, 2) computing of the functional STN by using an algorithm for calculation of the PFA, and 3) statistical analysis of the functional STN.

Several components of our method have already been described in detail in our previous work. The data acquisition and stereotactic environment have been presented in Reference 4. Several articles have addressed the surgical procedure (1–3, 5, 12) and neurological assessment, including selection of the clinically most effective contacts of stimulating electrodes (6, 9–11, 20, 21). The concept of the PFA was introduced in Reference 17. The algorithm for PFA generation is detailed in Reference 16. In addition, a web-enabled, public domain tool for PFA generation with data selection capabilities is presented in Reference 15.

Data Collection

To acquire the electrophysiological data, a five-channel device ("Ben-gun"; Integrated Surgical Systems, Lyon, France) was used under stereotactic conditions. It simultaneously guides five electrodes that are 2 mm apart from each other. The stereotactic frame is permanently positioned at the intersection focus of two orthogonal teleradiological x-ray tubes (3.5 m distance from the tubes to the x-ray films). Special care is taken to position the patient such that the midsagittal plane is parallel to the lateral projection plane as accurately as possible. For every patient, brain-specific and electrode-specific data are measured with 0.2- to 0.3-mm accuracy on two lateral and anteroposterior x-rays. Correction of the magnification coefficients is made, knowing the fixed geometry of the installation. This is additionally checked during calculation of the PFA (see the Discussion section).

The brain-specific data contain the locations of the posterior commissure (PC) and anterior commissure (AC), height of the thalamus (HT), and width of the third ventricle (V3) measured from the midline at the level of the target obtained from the ventriculographic x-rays performed before the electrode implantation session. The electrode-specific data comprise the positions of the deep brain stimulations and their best (clinically most effective) contacts obtained from the final control x-rays taken at the end of the implantation session. After surgery, the electrodes (in this study, all electrodes used were DBS 3389; Medtronic) are then connected to a chronically implanted programmable pacemaker (Kinetra; Medtronic). The best contact, selected out of four on the basis of the improvement of the symptoms akinesia, rigidity, and tremor (1), is determined for each, right and left, electrode by the neurological team after 3 months of follow-up. All outcomes were taken without having a threshold for selection; however, the global outcome (judged on the Unified Parkinson's Disease Rating Scale III, which is the motor score, maximum 108) of these patients was very good (65% improvement), and the SD was narrow (approximately 5% on the globality of items) (9).

Atlas Construction

The atlas constructed here is the PFA for the STN. To build this atlas, the data for each patient have to be normalized and placed in the same (common) atlas space. Data normalization uses linear scaling and shifting operations only. The atlas is calculated in a Cartesian coordinate system (x, y, z), where x is the anteroposterior axis passing through the PC and AC and having the PC as the origin; y is the lateral axis passing through the PC; and z is the dorsoventral axis passing through the PC. The x axis is scaled such that the distance between the PC and AC is 24 mm. The z axis is scaled such that the HT is 16 mm. The PFA is constructed from the best contacts only. The positions of these contacts are reconstructed from two orthogonal ventriculography x-rays and placed in the atlas space by application of linear scaling. This scaling is performed with respect to the available anatomic landmarks taken from the individual MRI scan (e.g., *Fig. 1, C–E*) or from the ventriculographic anteroposterior and lateral x-ray images. The "atlas function" at a given point in the stereotactic space is computed as the number of best contacts at this point. The probability is then calculated by linear scaling of the atlas function.

The surgical planning procedure (1–3, 5, 12) is based on the robust landmarks determined from ventriculography x-ray images: the AC, PC, HT, and V3. The spatial scaling used in our algorithm follows the concept of the surgical planning procedure. The coordinates of the best contacts are scaled anteroposteriorly proportionally to the intercommissural distance AC–PC and dorsoventrally proportionally to the HT. Lateral compensation against the width of the third ventricle was performed by shifting the y coordinate by $(V3_{average} - V3_{data})/2$, where V3 denotes the width of the third ventricle

measured from the midline at the axial level of the target. Two sets or results (with and without lateral compensation) were generated.

Because the approach has to be efficient for a large number of contacts, a fast and optimal algorithm for PFA calculation has been developed (16) and made available over the Internet (15, 27).

Probability Calculation

Probability is a linear function of the atlas. Probability $P(x, y, z)$ at point (x, y, z) is calculated as $P(x, y, z) = a(x, y, z)$, where $a(x, y, z)$ denotes the atlas function at point (x, y, z) and C is some constant. Probability may be useful for atlas interpretation, particularly if presented in image form. For instance, when C is the total number of best contacts, the probability gives the fraction of the contacts at a given location to the total number of contacts used to study the STN. When C is the maximum value of atlas function, the probability indicates the fraction of best contacts at a given location to the maximum number of best contacts overall in all locations in the STN. These definitions do not fulfill the mathematical definition of probability, although they may be useful practically. When C is the integral of atlas function over the whole atlas space, then probability is defined in a mathematical sense.

Material Selection

This study was performed for 168 bilateral cases with a single best contact only per electrode. This facilitates comparison of results for the STNL and STNR. In addition, we eliminated the cases the accuracy of which was outside the quality threshold of 0.25 mm (i.e., the same value as that of the atlas sampling step). The sources of this inaccuracy are addressed in the Discussion. The calculated actual height of the contact was compared with the known real one (1.5 mm), and cases with the contact absolute difference greater than 0.25 mm were rejected.

Computation of the Functional STN

By applying the PFA construction algorithm to the selected bilateral data, the probabilistic functional STN was calculated from 168 bilateral cases (336 best contacts) as an isotropic volume with an 0.25-mm sampling step (*Figs. 2* and *3*). The maximum values of the atlas function are 1) 36 for the STNL and 30 for the STNR without lateral compensation and 2) 33 for the STNL and 31 for the STNR with lateral compensation. Hence, when calculating probability, the constant C was set to 30, i.e., to the minimum of the highest values of the atlas.

The probabilistic functional volume of the structure, or in brief, functional volume, is a new measure introduced here for studying properties of the functional STN. It gives the relationship between a given probability P and the corresponding functional volume V and is denoted by $V(p)$. The functional volume $V(p)$ is defined as the volume of a region every point of which has a probability equal to or greater than p, where $p \in (0,1)$. The functional volume has the following properties: 1) the whole functional volume of the structure is obtained for the minimal probability (i.e., that corresponding to the atlas function value equal to 1); and 2) for $p_2 \geq p_1$, partial volumes $V(p_1)$, $V(p_2)$ satisfy $V(p_2) \subseteq V(p_1)$.

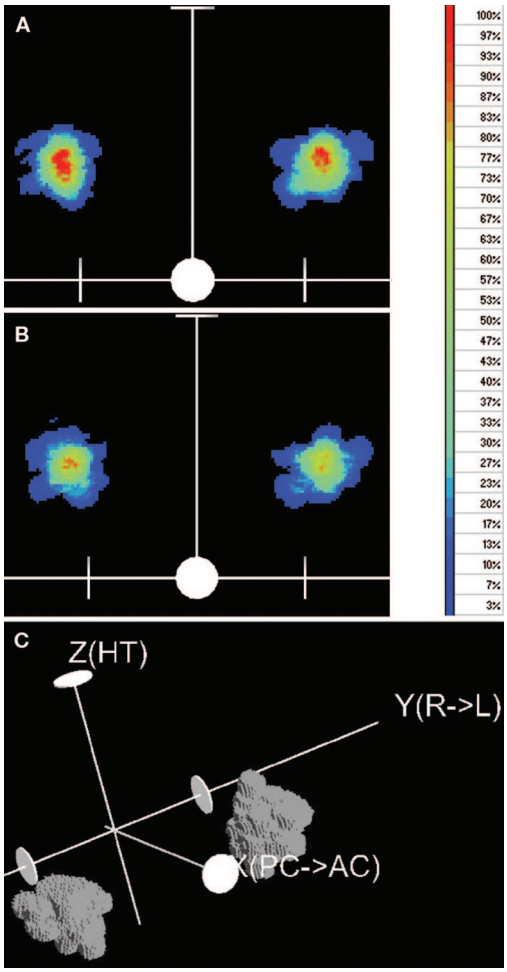

FIGURE 2. *Probabilistic functional STN calculated with 0.25-mm³ resolution without lateral compensation against the width of the third ventricle.* A, *axial section passing through the MV (the STNL is on the* left *side) and* (B) *axial section passing 0.5 mm above the MV; the probability color map is shown on the* right. C, *three-dimensional volumetric view. The origin of the coordinate system is at the PC. The* rings *(in all images) mark the positions of the AC on the* x *axis, HT on the* z *axis, and −10- and +10-mm distances laterally on the* y *axis.*

RESULTS

Basic features of the functional STN have been calculated for each hemisphere, including the location (atlas coordinates) of MV, SD, and size of functional volume (V) in cubic millimeters. In addition, the differences between these quantities for the STNL and STNR have been computed. Two sets of results have been calculated: 1) without lateral compensation

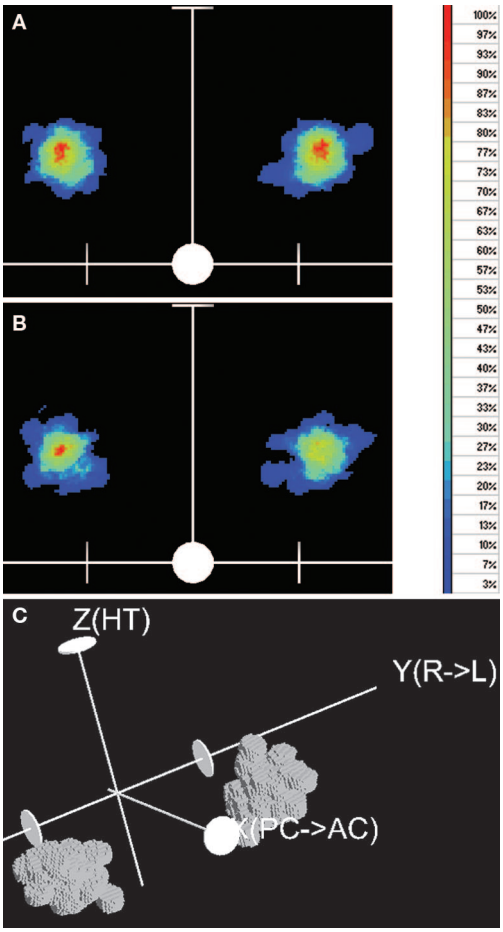

FIGURE 3. *Probabilistic functional STN calculated with 0.25-mm³ resolution with lateral compensation against the width of the third ventricle.* A, *axial section passing through the MV (the STNL is on the* left *side) and* B, *axial section passing 0.5 mm above the MV; the probability color map is shown on the* right. C, *three-dimensional volumetric view. The origin of the coordinate system is at the PC. The* rings *mark the positions of the AC on the* x *axis, HT on the* z *axis, and −10- and +10-mm distances laterally on the* y *axis.*

against the width of the third ventricle (*Table 1*) and 2) with lateral compensation (*Table 2*).

The coordinates of the best targets for the STNL and STNR are given in *Table 3* (without lateral compensation) and *Table 4* (with lateral compensation). For each hemisphere, these coordinates are calculated at the centers of the voxels (of 0.25 × 0.25 × 0.25 mm³ size) having the maximum atlas value.

We have also calculated the functional volumes for the STNL and STNR without lateral compensation (*Fig. 4*). Because *Figure 4* does not capture clearly any differentiation between the STNL and STNR, we have also computed the functional volume ratio $V_L(p)/V_R(p)$, where L (R) denotes the left (right) hemisphere (*Fig. 5*). Because the relationship in *Figure 5* is important, it is repeated for the laterally compensated atlas in *Figure 6*.

DISCUSSION

Influence of Surgical Procedure on Statistical Results

During the surgical procedure, both hemispheres were operated on in the same way, excluding the positioning of the bilateral electrodes. The mean angles of electrode insertion for the bilateral electrodes are almost the same, because the difference between them is only 0.33 degrees (*Table 1*), which is very low considering the geometry of a stimulating electrode (the diameter of contact is 1.2 mm, contact height is 1.5 mm, and intercontact gap is 0.5 mm). This is not surprising, because the track of insertion was calculated on the basis of the ventricular landmarks, which mean a symmetrical planned trajectory for each given patient. In this series, most of the time, the trajectory was not changed so as to avoid cortical structures such as veins.

Data Selection

Multiple criteria can be applied to choose a suitable set of cases for PFA generation to ensure its high quality and required properties. In an ideal case, the length of a physical electrode shall be equal to that reconstructed from two orthogonal projections, which condition is checked by the algorithm for PFA generation. There are various sources of potential errors and inaccuracy, such as low-accuracy measurement of the distances on the x-rays, wrong electrode type assigned, or inaccurate positioning of the patient. The more the patient's head is mispositioned, the more different the physical and reconstructed electrode lengths may be. Therefore, the PFA algorithm reconstructs the height of contact in three dimensions from its two projections. Because the physical height of contact is known (1.5 mm), an accuracy threshold can be set and only these contacts selected for which the reconstructed size is sufficiently close to its original value. This allows for balancing between the number of contacts used for PFA generation and their accuracy. For this study, we have rejected all cases for which the reconstructed contact height was smaller than 1.25 mm and larger than 1.75 mm, after x-ray magnification coefficient has been applied.

STN Features

The statistical analysis performed here examines standard features, such as location of MV and SD. In addition, a new feature, the probabilistic functional volume, has been introduced. Numerous measures have been tried that could potentially capture properties of the functional STN, and the functional volume has proved to be robust enough across various populations of best contacts as opposed to other measures. It gives a relationship between probability and the corresponding functional volume and enables us to study properties of the entire STN as well as to compare its left and right nuclei. It should be emphasized that

TABLE 1. Summary of findings for the functional subthalamic nucleus without lateral compensation against the width of the third ventricle[a]

Feature	Left STN	Right STN	Difference left versus right	Method of difference calculation
Number of best contacts, N	168	168	0	$N_L - N_R$
Maximum value of atlas, MAX	36	30	6	$MAX_L - MAX_R$
Normalized mean angle of electrode insertion, $\omega = (\omega_x, \omega_y, \omega_z)$	(62.79°, 90°−9.39°, 29.05°)	(62.89°, 90°+9.71°, 29.07°)	0.33°	$180\frac{arccos(\omega^L\omega^R)}{\pi}$ (the absolute values of y coordinate of the vectors are used)
Volume V_{whole} in mm^3	240.17	228.92	4.68%	$\frac{\lvert V_L - V_R\rvert}{V_L}100\%$
Volume of hot STN, V_{hot}, in mm^3	5.52	3.92	28.90%	$\frac{\lvert V_L - V_R\rvert}{V_L}100\%$
V_{hot}/V_{whole}	0.023	0.017	1.34	$\frac{V_{hot\ left}/V_{whole\ left}}{V_{hot\ right}/V_{whole\ right}}$
Location of mean value, $\mu = (\mu_x, \mu_y, \mu_z)$	(10.31, 11.62, −2.43)	(10.45, −11.49, −2.67)	0.31	$\sqrt{(\mu_x^L - \mu_x^L)^2 + (\lvert\mu_y^L\rvert - \lvert\mu_y^R\rvert)^2 + (\mu_z^L - \mu_z^R)^2}$
Location of mean value in hot STN, $h = (h_x, h_y, h_z)$	(10.34, 11.49, −2.72)	(10.57, −11.41, −2.76)	0.25	$\sqrt{(h_x^L - h_x^R)^2 + (\lvert h_y^L\rvert - \lvert h_y^R\rvert)^2 + (h_z^L - h_z^R)^2}, P \geq 0.77$
Standard deviation, $\sigma = (\sigma_x, \sigma_y, \sigma_z)$	(1.48, 1.27, 1.34)	(1.38, 1.41, 1.29)	0.18	$\sqrt{(\sigma_x^L - \sigma_x^R)^2 + (\sigma_y^L - \sigma_y^R)^2 + (\sigma_z^L - \sigma_z^R)^2}$

[a] STN, subthalamic nucleus.

functional volume is not a physical volume of structure; likewise, the PFA does not contain images of brain function.

Results without Lateral Compensation

MVs and SDs for the STNL and STNR are shown in *Table 1*. The MV difference is 0.31 mm and that for the SD is 0.18 mm, which is at the level of atlas resolution (that is, 0.25 mm). In absolute terms, the ratio of MV difference to the distance between MVs is 0.013. The differences between both STNs are less than 0.4 mm for MVs and approximately 0.2 mm for SDs. These results were further analyzed statistically by use of the SAS package (24), and details are given in the Appendix. This analysis indicates that the difference between the MVs of the STNL and STNR is significant in either situation (i.e., with and without lateral compensation).

The localization of the functional STN with respect to midsagittal plane is 11.62 ± 1.27 mm for the STNL and 11.49 ± 1.41 mm for the STNR. For comparison, the structural STN is located farther lateral, at 12.65 ± 1.3 mm, on the basis of 35 T2-weighted MRI scans (8). This means that the MRI-based targeting (8, 23) and PFA-based targeting for subthalamic stimulation planning result in two different initial targets. Because PFA is based on neuroelectrophysiology (both microrecording and clinical evaluation of the beneficial effects of microstimulation), it may be superior to MRI-based targeting.

Several measures used here indicate some differences between the STNL and STNR, particularly without lateral compensation. Statistically, in either situation, the difference between the MVs for the STNL and STNR is significant (see the Appendix). The maximum atlas value of the STNL is greater by 6 than that of the STNR (*Table 1*), which is 20% more. The size of the functional STN volume (corresponding to the entire range of probabilities) is 240.17 mm^3 for the STNL and 228.92 mm^3 for the STNL (*Table 1*). For comparison, the anatomic STN volume approximated from the Schaltenbrand-Wahren brain atlas (25) is 183 mm^3. In addition, the images of STNL look "hotter" than those of STNR (*Fig. 2*).

The functional volume ratio $V_L(p)/V_R(p)$ (*Fig. 5*) shows two behaviors. For low and medium probabilities, the corresponding functional volume ratio is nearly constant. However, from a certain probability, there is an increasing difference between the STNL and STNR. The probability that divides the functional volume ratio $V_L(p)/V_R(p)$ graph into the nearly linear section and the approximately exponential section is taken as that separating the functional STN into two parts. We call them the *cold STN* and *hot STN* according to the color scale used to map probability to color. Quantitatively, this probability is taken as the value that gives a substantial increase. This increase, clearly observable on the functional volume ratio graph, is 24% in our study, which corresponds to a probability of $P = 0.77$.

The hot STNL is 1.41 times larger and 20% more dense that the hot STNR. In addition, for a given probability, the corresponding functional volume for the hot STNL is up to 43 times larger than that for the hot STNR, reaching the maximum ratio of 43 for $P = 1.0$ (*Fig. 5*).

Results with Lateral Compensation

Lateral compensation (*Table 2*) results in a higher lateral SD (spread). Conversely, the differences between the STNL and

TABLE 2. Summary of findings for the functional subthalamic nucleus with lateral compensation against the width of the third ventricle[a]

Feature	Left STN	Right STN	Difference left versus right	Method of difference calculation
Number of best contacts, N	168	168	0	$N_L - N_R$
Maximum value of atlas, MAX	33	31	2	$MAX_L - MAX_R$
Normalized mean angle of electrode insertion, $\omega = (\omega_x, \omega_y, \omega_z)$	(62.79°, 90°−9.39°, 29.05°)	(62.89°, 90°+9.71°, 29.07°)	0.33°	$180\frac{arccos(\omega^L\omega^R)}{\pi}$ (the absolute values of y coordinate of the vectors are used)
Volume V_{whole} in mm^3	249.88	249.86	0.01%	$\frac{V_L - V_R}{V_L}100\%$
Volume of hot STN, V_{hot}, in mm^3	3.33	3.61	8.41%	$\frac{V_L - V_R}{V_L}100\%$
V_{hot}/V_{whole}	0.013	0.014	0.92	$\frac{V_{hot\ left}/V_{whole\ left}}{V_{hot\ right}/V_{whole\ right}}$
Location of mean value, $\mu = (\mu_x, \mu_y, \mu_z)$	(10.31, 12.06, −2.43)	(10.45, −11.93, −2.67)	0.31	$\sqrt{(\mu_x^L - \mu_x^L)^2 + (\lvert\mu_y^L\rvert - \lvert\mu_y^R\rvert)^2 + (\mu_z^L - \mu_z^R)^2}$
Location of mean value in hot STN, $h = (h_x, h_y, h_z)$	(10.60, 12.39, −2.61)	(10.60, −11.94, −2.69)	0.46	$\sqrt{(h_x^L - h_x^R)^2 + (\lvert h_y^L\rvert - \lvert h_y^R\rvert)^2 + (h_z^L - h_z^R)^2}, P \geq 0.77$
Standard deviation, $\sigma = (\sigma_x, \sigma_y, \sigma_z)$	(1.48, 1.44, 1.34)	(1.38, 1.53, 1.29)	0.14	$\sqrt{(\sigma_x^L - \sigma_x^R)^2 + (\sigma_y^L - \sigma_y^R)^2 + (\sigma_z^L - \sigma_z^R)^2}$

[a] STN, subthalamic nucleus.

TABLE 3. The coordinates (in mm) of best targets for the left and right subthalamic nucleus without lateral compensation[a]

	Coordinate *x*	Coordinate *y*	Coordinate *z*	Atlas value *a(x,y,z)*
Left functional STN	10.00	11.25	−3.00	36
	10.00	11.25	−2.75	36
	10.00	11.50	−2.75	36
	10.00	11.75	−2.75	36
Right functional STN	11.25	−11.50	−2.75	30
	11.50	−11.50	−2.50	30

[a] STN, subthalamic nucleus.

STNR are reduced. The relative value of the absolute difference between the whole functional volumes is only 0.01%, and that between the hot volumes is 8.1%. Qualitatively, almost similar findings are observed. The hot STN can be distinguished by analyzing the functional volume ratio graph. Similarly, in the hot STN, for the same probability, the functional volume of the STNL is (equal to or) greater than that of the STNR. The higher the probability, the greater the ratio of the functional STNL to the STNR (*Fig. 6*). The highest ratio is 11 versus 43 obtained for the atlas without compensation of laterality. However, in both cases, i.e., with and without lateral compensation, the size of the hot STN in comparison to the whole STN remains very small, between 1 and 2% (*Fig. 7*).

Limitations

The method presented has several limitations that are primarily a result of data acquisition and PFA generation. The data used for this study are limited to PD patients. The invasiveness of the procedure does not permit performing it for normal subjects to compare the results. Because the data are originating from the group that pioneered bilateral subthalamic stimulation, there might be a bias introduced by the unicity of this single center and by their specific practices of performing surgical procedure, neurological assessment, and selection of the best contacts to improve the symptoms of akinesia, rigidity, and tremor.

The PFA uses a simplified modeling of a functional region corresponding geometrically to the contact shape and ignor-

TABLE 4. The coordinates (in mm) of best targets for the left and right subthalamic nucleus with lateral compensation[a]

	Coordinate *x*	Coordinate *y*	Coordinate *z*	Atlas value *a(x,y,z)*)
Left functional STN	10.25	12.25	−2.75	33
Right functional STN	11.00	−12.30	−2.75	31

[a] STN, subthalamic nucleus.

ing the complex interaction between the stimulating electrode and the surrounding tissues. Moreover, patient data normalization is limited to two linear scalings along the anteroposterior and dorsoventral axes and the lateral shift. A three-dimensional nonlinear warping is theoretically superior, but it would require three-dimensional neuroimage data acquisition, such as MRI, which would substantially reduce the accuracy obtained with the present approach (i.e., 0.25 mm) because of geometric distortions and limited spatial resolution. All these simplifications, however, permit hundreds of contacts to be processed rapidly to generate the PFA, which enables quick PFA updates.

It should be emphasized that the PFA and functional volume are new concepts and that the calculated functional STN cannot be linked directly to a physical STN. The functional STN considered here shows a normalized spatial distribution of the best contacts from bilateral subthalamic stimulation procedures selected to improve the symptoms of akinesia, rigidity, and tremor. This work, however, does not give the probability for the real boundaries of the STN or the location of its known components, such as the sensorimotor part of the STN.

Clinical Usefulness

A potential usefulness of the results obtained here is in atlas-based planning of subthalamic stimulation procedures. The current practice is to use electronic versions of print brain atlases (such as Schaltenbrand-Wahren [25] or Talairach-Tournoux [26]) available in most packages for stereotactic and functional neurosurgery (17). These atlases allow only the delineation of the target structure without specifying the target point. In addition, they have several limitations, as discussed in Reference 13. PFA-based planning may be superior to the current practice, because it is more precise and provides the unique target point (or points) in the stereotactic space (*Tables 3* and *4*). The PFA has to be individualized first by performing the inverse transformation to that used for its creation. Then, the best-planned target is the point in the individualized atlas with the highest probability of being the best target on the basis of the patients previously operated on. Because the best target is in the hot STN, the size of the hot STN determines the precision of targeting. This size in comparison to the size of whole STN remains very small, between 1 and 2% of the whole functional volume (*Tables 1* and *2*; *Fig. 7*), independently of applying lateral compensation or lack thereof. Therefore, target planning and execution have to be performed with high precision. To facilitate PFA-based planning of subthalamic stimulations, the functional STN atlas was coregistered spatially with the Schaltenbrand-Wahren atlas (14), and a dedicated application has been developed (18) (*Fig. 8*).

We believe that the method presented is general enough and applicable not only to human but also to animal studies. Because numerous centers are currently gathering large amounts of electrophysiological human and animal data, the present work may potentially open new avenues in exploiting these data. Its potential use is facilitated by the public availability of the algorithm for PFA generation (at www.cerefy-.com). In addition, the functional volume is a useful measure characterizing probabilistic functional distribution of the best contacts. We hope that this work may trigger more efforts to use the PFA and functional volume concepts. This may result in generating the PFA for other specific structures than the STN with the best contacts selected for various criteria and to improve other symptoms than those studied here.

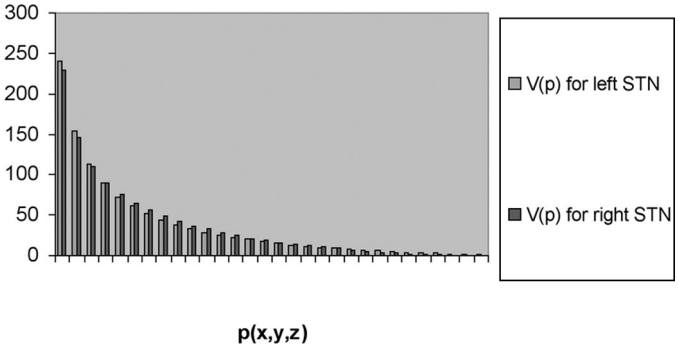

FIGURE 4. *Volume* V(p) *for the STNL and STNR calculated without lateral compensation against the width of the third ventricle.* V(p) *is calculated for all voxels having probability* P *or higher.*

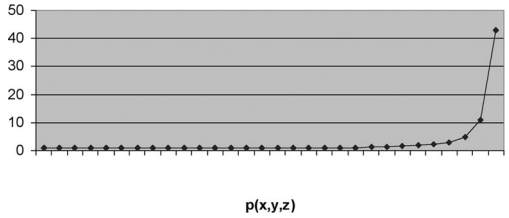

FIGURE 5. *Volume differences between the STNL and STNR calculated without lateral compensation against the width of the third ventricle:* $V_L(p)/V_R(p)$ *ratio in function of probability.*

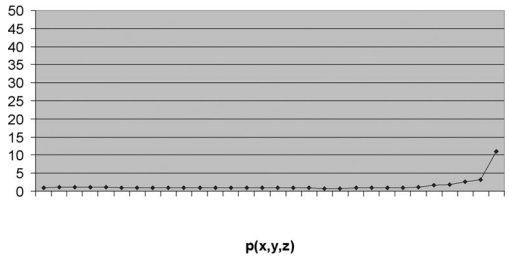

FIGURE 6. *Volume differences between the STNL and STNR calculated with lateral compensation against the width of the third ventricle:* $V_L(p)/V_R(p)$ *ratio in function of probability. The scale is the same as in Figure 5 for better comparison.*

CONCLUSIONS

This work provides an attempt to study the results of a large number of bilateral subthalamic stimulations from a probabilistic standpoint. By analyzing data for the patients previously operated on, some conclusions about the most probable stereotactic targets for the patients to be operated on can be drawn and come in addition to the other efforts developed during the surgical procedure to achieve the best electrode placement.

This article introduces a method for studying the functional properties of subcortical structures from a large electrophysiological and neuroimaging data set by means of the PFA. The PFA provides a spatial distribution of the clinically most effective contacts normalized to the common atlas space. Practically, the PFA is a dynamic map of functional properties of cerebral structures that can be recalculated rapidly in a few seconds and updated with the new patients.

The statistical analysis of the PFA not only allows the calculation of such typical features as MV and SD but also provides the probability distribution and, particularly, the distribution of regions with the highest probability. As a result, we have identified within the STN a region of high probability called the hot STN. In the hot STN, for the same probability, the functional volume of the STNL is larger than that of the STNR. The higher the probability, the greater the volume ratio of the functional STNL to the STNR. This tendency holds independently of whether the contacts are laterally compensated or not against the width of the third ventricle, although in case of lateral compensation, this differentiation is lower.

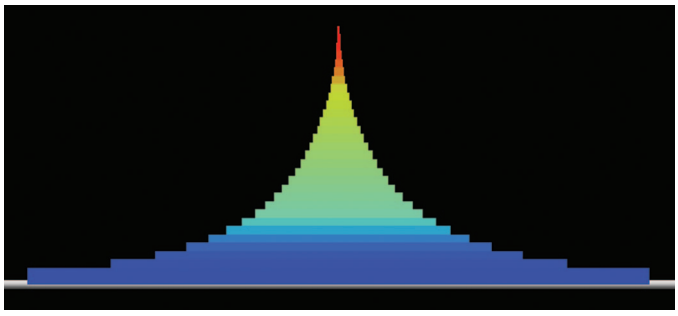

FIGURE 7. *Probability distribution histogram of the STN calculated without lateral compensation against the width of the third ventricle (the probability color bar is the same as those in Figs. 2* and *3). The length of each horizontal level (*bar*) is proportional to the atlas volume (the number of voxels) that contain the number of best contacts equal to this level number (starting from one best contact at the* bottom*, two best contacts in the* second level*, and so on). Note that the high-probability volume (at the* top *of the histogram) is very small in comparison to the low-probability volume (at the* bottom *of the histogram).*

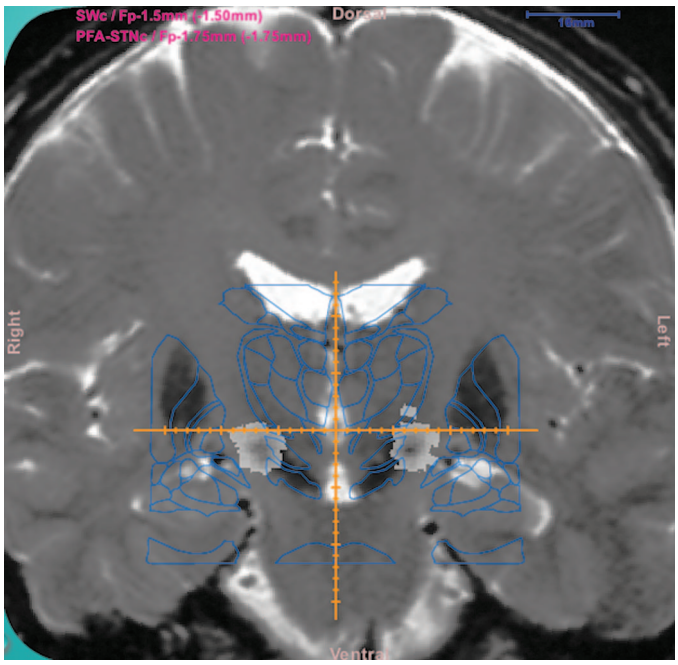

FIGURE 8. *A T2-weighted coronal MRI scan with the PFA and Schaltenbrand-Wahren atlas overlaid on it. The PFA is shown as a* gray-scale image *with the intensity inversely proportional to probability (the* black *denotes probability = 1.0). The reference axes have marks at every 2 mm.*

Although this is still a method belonging to the "indirect targeting," PFA-based planning may be superior to the current practice based on crude ratios of basic landmarks such as AC–PC distance and HT, because it is more precise and provides a unique, statistically weighted target point in the stereotactic space (particularly when the individualized PFA can be displayed together with the MRI scans (for the teams practicing the so-called direct anatomic targeting) and the electronic anatomic atlas (18). Then, the best PFA-based stereotactic target is the point in the individualized atlas with the highest probability of being the best target for the previously operated patients. Because the best target is in the hot STN, the size of the hot STN determines the precision of targeting. The methodology presented based on the PFA and functional volume is general and can be applied to study not only the STN for PD treatment but also other structures, with the best contacts selected for various criteria and symptoms.

```
[Statistics] - name of used method calculating multivariate analog of the t-statistics
[Value] - value calculated by the method
[F Value] - corresponding value F distributed
[Num DF] - numerator degrees of freedom (in our case of 3D points, so it is 3)
[Den DF] - denominator degrees of freedom (in our case it is a number of 3D points in both
groups)
<.0001 means that value of probability density of F distribution at [F value] is less than 0.0001
```

Comparing the left and right mean vectors with lateral compensation

Statistic	Value	F Value	Num DF	Den DF	Pr > F
Wilks' Lambda	0.98622576	640.33	3	137541	<.0001
Pillai's Trace	0.01377424	640.33	3	137541	<.0001
Hotelling-Lawley Trace	0.01396662	640.33	3	137541	<.0001
Roy's Greatest Root	0.01396662	640.33	3	137541	<.0001

Comparing the left and right mean vectors without lateral compensation

Statistic	Value	F Value	Num DF	Den DF	Pr > F
Wilks' Lambda	0.98547221	675.35	3	137434	<.0001
Pillai's Trace	0.01452779	675.35	3	137434	<.0001
Hotelling-Lawley Trace	0.01474196	675.35	3	137434	<.0001
Roy's Greatest Root	0.01474196	675.35	3	137434	<.0001

FIGURE 9. *Definitions and statistical analysis.*

Acknowledgments

We thank Dr. Alexander Weissman for his help with SAS. The work on algorithm development and data analysis was funded by the Biomedical Research Council of the Agency for Science, Technology, and Research, Singapore.

APPENDIX

Appendix: statistical analysis

The multivariate *t* tests (22) including Wilks' Lambda, Pillai's Trace, Hotelling-Lawley Trace, and Roy's Greatest Root statistics (22) were performed using SAS software (24). The results showed that the mean vectors of the functional STNL and STNR with and without lateral compensation were significantly different. It also proved that the distributions presented by the functional STNL and STNR were significantly different with or without lateral compensation.

Both cases with and without lateral compensation were considered (see below, output from SAS). For each case, two hypotheses, H0 (the difference between the mean vectors is not significant) and H1 (the difference between the mean vectors is significant), were checked between two sets of three-dimensional points (from the left and right hemispheres), where each point **(***x*, *y*, *z***)** had a frequency that equaled the atlas value a**(***x*, *y*, *z*). The size of each set exceeded 68,000 points. To make the sets comparable, the second coordinate *y* was substituted with its absolute value. The observed values of the statistics in multivariate (with lateral compensation of 640.33 and without lateral compensation of 675.35) tests correspond to the probability density of the statistics (F distribution) that is lower than 0.0001 (*Fig. 9*), which immediately rejects hypothesis H0 and accepts H1 under any significance level greater than 0.0001.

REFERENCES

1. Benabid AL, Koudsie A, Benazzouz A, Fraix V, Ashraf A, Le Bas JF, Chabardes S, Pollak P: Subthalamic stimulation for Parkinson's disease. **Arch Med Res** 31:282–289, 2000.
2. Benabid AL, Koudsie A, Pollak P, Kahane P, Chabardes S, Hirsch E, Marescaux C, Benazzouz A: Future prospects of brain stimulation. **Neurol Res** 22:237–246, 2000.
3. Benabid AL, Krack PP, Benazzouz A, Limousin P, Koudsie A, Pollak P: Deep brain stimulation of the subthalamic nucleus for Parkinson's disease: Methodologic aspects and clinical criteria. **Neurology** 55[Suppl 6]:S40–S44, 2000.
4. Benabid AL, Lavallee S, Hoffmann D, Cinquin P, Le Bas JF, Demongeot J: Computer support for the Talairach system, in Kelly PJ, Kall BA (eds): *Computers in Stereotactic Neurosurgery*. Boston, Blackwell, 1992, pp 230–245.
5. Benabid AL, Pollak P, Gross C, Hoffmann D, Benazzouz A, Gao DM, Laurent A, Gentil M, Perret J: Acute and long-term effects of subthalamic nucleus stimulation in Parkinson's disease. **Stereotact Funct Neurosurg** 62:76–84, 1994.
6. Charles PD, Van Blercom N, Krack P, Lee SL, Xie J, Besson G, Benabid AL, Pollak P: Predictors of effective bilateral subthalamic nucleus stimulation for PD. **Neurology** 59:932–934, 2002.
7. DeLong MR: Primate models of movement disorders of basal ganglia origin. **Trends Neurosci** 13:281–285, 1990.
8. Hamel W, Zhu XL, Schrader B, Weinert D, Hedderich J, Muller D, Mehdorn HM: Magnetic resonance imaging-based morphometry and landmark correlation of basal ganglia nuclei. Proceedings of the 53rd Annual Meeting of the German Society of Neurosurgery, Halle/Saale, June 2–5, 2002 (DI.01.04).
9. Krack P, Batir A, Van Blercom N, Chabardes S, Fraix V, Ardouin C, Koudsie A, Limousin PD, Benazzouz A, Le Bas JF, Benabid AL, Pollak P: Five-year follow-up of bilateral stimulation of the subthalamic nucleus in advanced Parkinson's disease. **N Engl J Med** 349:1925–1934, 2003.

10. Krack P, Fraix V, Mendes A, Benabid AL, Pollak P: Postoperative management of subthalamic nucleus stimulation for Parkinson's disease. **Mov Disord** 17[Suppl 3]:S188–S197, 2002.
11. Lagrange E, Krack P, Moro E, Ardouin C, Van Blercom N, Chabardes S, Benabid AL, Pollak P: Bilateral subthalamic nucleus stimulation improves health-related quality of life in PD. **Neurology** 59:1976–1978, 2002.
12. Limousin P, Pollak P, Benazzouz A, Hoffmann D, Broussolle E, Perret JE, Benabid AL: Bilateral subthalamic nucleus stimulation for severe Parkinson's disease. **Mov Disord** 10:672–674, 1995.
13. Nowinski WL: Computerized brain atlases for surgery of movement disorders. **Semin Neurosurg** 12:183–194, 2001.
14. Nowinski WL: Co-registration of the Schaltenbrand-Wahren microseries with the probabilistic functional atlas. **Stereotact Funct Neurosurg** 82:142–146, 2004.
15. Nowinski WL, Belov D, Benabid AL: A community-centric Internet portal for stereotactic and functional neurosurgery with a probabilistic functional atlas. **Stereotact Funct Neurosurg** 79:1–12, 2002.
16. Nowinski WL, Belov D, Benabid AL: An algorithm for rapid calculation of a probabilistic functional atlas of subcortical structures from electrophysiological data collected during functional neurosurgery procedures. **NeuroImage** 18:143–155, 2003.
17. Nowinski WL, Benabid AL: New directions in atlas-assisted stereotactic functional neurosurgery, in Germano IM (ed): *Advanced Techniques in Image-Guided Brain and Spine Surgery*. New York, Thieme, 2002, pp 162–174.
18. Nowinski WL, Thirunavuukarasuu A, Benabid AL: *The Cerefy Clinical Brain Atlas: Extended Edition with Surgery Planning and Intraoperative Support*. New York, Thieme, 2005.
19. Plenz D, Kitai S: A basal ganglia pacemaker formed by the subthalamic nucleus and external globus pallidus. **Nature** 400:677–682, 1999.
20. Pollak P, Fraix V, Krack P, Moro E, Mendes A, Chabardes S, Koudsie A, Benabid AL: Treatment results: Parkinson's disease. **Mov Disord** 17[Suppl 3]:S75–S83, 2002.
21. Pollak P, Krack P, Fraix V, Mendes A, Moro E, Chabardes S, Benabid AL: Intraoperative micro- and macrostimulation of the subthalamic nucleus in Parkinson's disease. **Mov Disord** 17[Suppl 3]:S155–S161, 2002.
22. Rencher AC: *Methods of Multivariate Analysis*. New York, John Wiley & Sons, 1995, p. 137.
23. Saint-Cyr JA, Hoque T, Pereira LC, Dostrovsky JO, Hutchison WD, Mikulis DJ, Abosch A, Sime E, Lang AE, Lozano AM: Localization of clinically effective stimulating electrodes in the human subthalamic nucleus on magnetic resonance imaging. **J Neurosurg** 97:1152–1166, 2002.
24. SAS Institute: SAS, version 8.0. Cary, SAS Institute, Inc., 1999.
25. Schaltenbrand G, Wahren W: *Atlas for Stereotaxy of the Human Brain*. Stuttgart, Thieme, 1977.
26. Talairach J, Tournoux P: *Co-Planar Stereotactic Atlas of the Human Brain*. Stuttgart, Georg Thieme Verlag/Thieme Medical Publishers, 1988.
27. http://www.cerefy.net/CPforSFN.html. Accessed July 12, 2005.

COMMENTS

This very interesting article explores the possibility of building a probabilistic atlas of the subthalamic nucleus (STN) region, and it demonstrates, in a very elegant way, that subcortical neuronal structures also have a dominant side. In addition, the authors discuss the whole philosophy of brain exploration and monitoring in the surgery of movement disorders.

A similar effort was performed by our group and presented at the London meeting of the European Society for Stereotactic and Functional Surgery in 2000. At that time, a criticism was raised by the audience claiming that the selection of patients had been done by use of a simple Boolean criterion including only patients who obtained a "good" clinical result. A similar pitfall seems to affect this article.

The expected results for this mathematical elaboration of clinical and neurophysiological data should be the immediate and prompt availability of the STN stereotactic coordinates, in which the probability to hit a target allowing for achieving a good clinical result is higher. Unfortunately, the probability of achieving a good clinical outcome leaving the electrode at the initial target determined by the algorithm illustrated in the article ("hot" STN of the AAs) is not easily intelligible. In addition, this article introduces and develops the (misleading?) concept that optimal clinical results may be derived by the mathematical elaboration of neuroimaging data. Because such an approach might lead to an easy and direct STN targeting procedure, this yields a questionable role for microrecording in routine procedures. Some more comments would have been expected about the future of neurophysiological exploration of the region of the STN by the group who popularized it. We think that the statistical need for a second or third electrode track, which some groups claim is always needed, should be made evident.

Despite these criticisms, we think that this article is really interesting for the neurosurgical community and that it will play an important role in the discussion about the possibility of reducing the clinical need for exploration and to optimize the initial target. The purely rationalistic galenian and newtonian approach to medical problems that dominated 19th- and 20-century medicine will probably be replaced in the future by a more comprehensive statistical and stochastic approach. Also, in the field of movement disorders as well as in the field of epilepsy (in which epileptologists are using the concept of networks to explain the genesis of the seizures and surgeons are adopting a disconnective attitude), the concept of a complex and interactive network is becoming more and more popular. The "hot" STN should perhaps be considered the node of the network involved in Parkinson's disease the manipulation of which is easiest and brings the best results.

Angelo Franzini
Giovanni Broggi
Milan, Italy

Individual anatomic variability has confounded stereotactic localization methods since the beginnings of human functional stereotactic surgery. Subcortical target structures have no constant relationship to radiologically determined landmarks, notably the commissures and the midline of the third ventricle. Some anatomic stereotactic atlases, such as that of Andrew and Watkins, for example, have used probability plots derived from data on multiple anatomic specimens to indicate where any specific anatomic structure has the greatest probability of being found within a stereotactic coordinate system on the basis of ventricular system landmarks. In this article, the authors attempt to do a similar thing with electrophysiological data: the clinical results produced by stimulation of a specific deep brain stimulation (DBS) electrode and its stereotactic location within a radiologically defined coordinate system. As I understand it, from these data, a map (atlas) is derived to indicate the probability of any specific coordinate point having a satisfactory clinical result. This information may help surgeons select the initial target for microelectrode recording corroboration and reduce the number of microelectrode passes required to confirm the anatomic target before placing the DBS electrode. However, I do not believe that a "probabilistic" atlas will render electrophysiological corroboration of subcortical targets unnecessary.

Patrick J. Kelly
New York, New York

This article carefully documents the locations of the most clinically effective electrode contacts for DBS in the region of the STN. Coming from the originators of STN DBS and drawn from a large

series of 168 leads, these data provide a rational, outcomes-driven formula for selecting the anatomic target for STN DBS.

The optimal contact for maximum clinical improvement was selected 3 months after implantation. These "best contacts" are plotted in a common space with the origin at the posterior commissure. Individual brains are normalized in the anteroposterior dimension with respect to anterior commissure-posterior commissure line length and in the vertical dimension with respect to thalamic height. Contact localization is derived from intraoperative ventriculography, performed in an operating suite that was specially designed for obtaining consistent x-ray projection angles to optimize ventriculographic measurements.

Most readers will find the key information in *Table 1* in the article, second line from the bottom. Here, the authors report mean coordinates for the cluster of active contacts. The data are plotted separately for left versus right contacts, although the mean coordinates are very similar for the two sides. These coordinates presumably reflect optimized clinical outcomes, because the choice of which contact to activate was based on neurological assessment of the effect of stimulation through each of the four available contacts. Most other published targeting strategies are derived from localizing the STN anatomically on brain atlases or on individual patients' brain magnetic resonance imaging scans or from post hoc analysis of the locations of microelectrode penetrations on which the motor territory of the STN was physiologically identified.

Comparison of the last row in *Tables 1* and *2* shows that the standard deviation of the mean contact coordinates did not decrease with mathematical compensation for width of the third ventricle (normalizing all lateral coordinates to mean third ventricular width). This suggests that adjustment of the lateral target coordinate for third ventricle width, often performed when targeting the thalamus or globus pallidus, may not be necessary for the STN. Furthermore, in anterior commissure-posterior commissure–based coordinates, the volume of the space with the most dense concentration of contacts (which these authors call "hot STN") is quite small. This suggests that anatomic variability in the optimal target point for STN DBS is fairly small. This contrasts with the globus pallidus, in which anatomic variability of a physiologically defined point is significant (1, 2).

The authors make the assumption a priori that the cluster of active contacts is within the STN. Others have argued that the optimal contact may be dorsal to the STN (3). It is thus an important result of this article that the coordinates of the most dense cluster of active contacts would in fact correspond to the STN itself rather than the region dorsal to it if plotted on standard human brain atlases or on most patients' brain magnetic resonance imaging scans.

The authors argue that there is a difference in the properties of the probabilistic atlas for left versus right brains. I was more impressed by the bilateral symmetry of the atlas than by its asymmetry. I do not think that these data prove a real difference in functional anatomy between the left and right STN, although the suggestion is an interesting one.

Philip A. Starr
San Francisco, California

---

1. Guridi J, Gorospe A, Ramos E, Linazasoro G, Rodriguez MC, Obeso JA: Stereotactic targeting of the globus pallidus internus in Parkinson's disease: Imaging versus electrophysiological mapping. **Neurosurgery** 45:278–289, 1999.
2. Starr PA; Vitek JL, DeLong M, Bakay RA: MRI-based stereotactic targeting of the globus pallidus and subthalamic nucleus. **Neurosurgery** 44:303–314, 1999.
3. Voges J, Volkmann J, Allert N, Lehrke R, Koulousakis A, Freund HJ, Sturm V: Bilateral high-frequency stimulation in the subthalamic nucleus for the treatment of Parkinson disease: correlation of therapeutic effect with anatomical electrode position. **J Neurosurg** 96:269–279, 2002.

Dr. Nowinski and colleagues have compiled a very large number of data points documenting the optimal target associated with clinical benefit in patients with Parkinson's disease undergoing bilateral STN stimulation. This work by the pioneering group in DBS surgery in the STN provides a useful compilation using a large data set outlining the location in the brain in relation to the commissures that is best correlated with a good clinical outcome. In this way, they have provided an important service to the neurosurgical community. This type of analysis can of course be expanded and performed with other targets, such as the globus pallidus and the thalamus for movement disorders and for other cortical and noncortical sites for the treatment of various disorders, including epilepsy, pain, and psychiatric illnesses. This approach may prove to be useful across many procedures in functional neurosurgery.

Andres M. Lozano
Toronto, Ontario, Canada